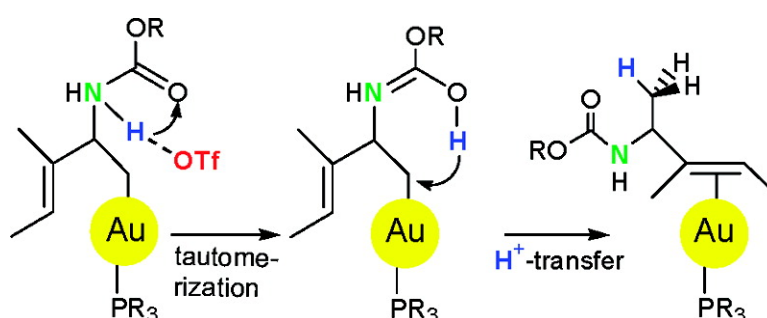


The Reaction Mechanism of the Hydroamination of Alkenes Catalyzed by Gold(I)–Phosphine: The Role of the Counterion and the N-Nucleophile Substituents in the Proton-Transfer Step

Gbor Kovcs, Gregori Ujaque, and Agust Lleds

J. Am. Chem. Soc., **2008**, 130 (3), 853-864 • DOI: 10.1021/ja073578i

Downloaded from <http://pubs.acs.org> on February 8, 2009



More About This Article

Additional resources and features associated with this article are available within the HTML version:

- Supporting Information
- Links to the 8 articles that cite this article, as of the time of this article download
- Access to high resolution figures
- Links to articles and content related to this article
- Copyright permission to reproduce figures and/or text from this article

[View the Full Text HTML](#)

The Reaction Mechanism of the Hydroamination of Alkenes Catalyzed by Gold(I)–Phosphine: The Role of the Counterion and the N-Nucleophile Substituents in the Proton-Transfer Step

Gábor Kovács,^{†,‡} Gregori Ujaque,^{*,†} and Agustí Lledós[†]

Departament de Química, Universitat Autònoma de Barcelona, 08193 Bellaterra, (Barcelona), Spain, and Research Group of Homogeneous Catalysis, Hungarian Academy of Sciences, Debrecen 10, P.O. Box 7, H-4010 Hungary

Received May 18, 2007; E-mail: gregori@klngon.uab.es

Abstract: The reaction mechanism of the gold(I)–phosphine-catalyzed hydroamination of 1,3-dienes was analyzed by means of density functional methods combined with polarizable continuum models. Several mechanistic pathways for the reaction were considered and evaluated. It was found that the most favorable series of reaction steps include the ligand substitution reaction in the catalytically active Ph_3PAuOTf species between the triflate and the substrate, subsequent nucleophile attack of the N-nucleophile (benzyl carbamate) on the activated double bond, which is followed by proton transfer from the NH_2 group to the unsaturated carbon atom. The latter step, the most striking one, was analyzed in detail, and a novel pathway involving tautomerization of benzyl carbamate nucleophile assisted by triflate anion acting as a proton shuttle was characterized by the lowest barrier, which is consistent with experimental findings.

Introduction

Homogeneous catalysis with gold complexes has been one of the most rapidly developing fields of organometallic catalysis in the last years.¹ Complexes having gold(I) or gold(III) metal centers had been historically considered not active or representing catalysts of inferior activity compared with other transition metal complexes. Nevertheless, this attitude has completely changed in the recent years, and several research groups have

dedicated much effort to explore gold-catalyzed homogeneous catalytic reactions.²

The catalysis of nucleophilic additions by gold complexes has been one of the most investigated reactions in modern organometallic catalysis.^{3–6} Gold complexes are Lewis acids that activate C–C multiple bonds toward nucleophilic attack. Earlier, platinum,⁷ ruthenium,⁸ and palladium⁹ complexes were shown to catalyze such reactions; however, these reactions were not efficient enough to take place under mild conditions. Among

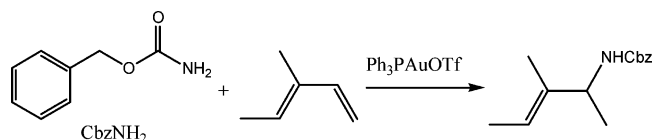
[†] Universitat Autònoma de Barcelona.

[‡] Hungarian Academy of Sciences.

- (1) Recent Reviews: (a) Hashmi, A. S. K. *Gold Bull.* **2004**, *37*, 51. (b) Echavarren, A. M.; Nevado, C. *Chem. Soc. Rev.* **2004**, *33*, 431. (c) Arcadi, A.; Di Giuseppe, S. *Curr. Org. Chem.* **2004**, *8*, 795. (d) Hoffmann-Röder, A.; Krause, N. *Org. Biomol. Chem.* **2005**, *3*, 387. (e) Hashmi, A. S. K.; Hutchings, G. J. *Angew. Chem., Int. Ed.* **2006**, *45*, 7896. (f) Ma, S.; Yu, S.; Gu, Z. *Angew. Chem., Int. Ed.* **2006**, *45*, 200. (g) Jimenez-Núñez, E.; Echavarren, A. M. *Chem. Commun.* **2007**, 333. (h) Hashmi, A. S. K. *Chem. Rev.* **2007**, *107*, 3180.
- (2) Some examples: (a) Ito, Y.; Sawamura, M.; Hayashi, T. *J. Am. Chem. Soc.* **1986**, *108*, 6405. (b) Skouta, R.; Li, C. J. *Angew. Chem., Int. Ed.* **2007**, *46*, 1117. (c) Dube, P.; Toste, F. D. *J. Am. Chem. Soc.* **2006**, *128*, 12062. (d) Casado, R.; Contel, M.; Laguna, M.; Romero, P.; Sanz, S. J. *Am. Chem. Soc.* **2003**, *125*, 11925. (e) Gonzalez-Arellano, C.; Abad, A.; Corma, A.; Garcia, H.; Iglesias, M.; Sanchez, F. *Angew. Chem., Int. Ed.* **2007**, *46*, 1536. (f) Arcadi, A.; Di Giuseppe, S.; Marinelli, F.; Rossi, E. *Adv. Synth. Catal.* **2001**, *343*, 443. (g) Zhang, Z. B.; Widenhoefer, R. A. *Angew. Chem., Int. Ed.* **2007**, *46*, 283. (h) Hildebrandt, D.; Dyker, D. J. *Org. Chem.* **2006**, *71*, 6728. (i) Hashmi, A. S. K.; Weyrauch, J. P.; Kurpejovi, E.; Frost, T. M.; Miehlich, B.; Frey, W.; Bats, J. W. *Chem. Eur. J.* **2006**, *12*, 5806. (j) Robles-Machín, R.; Adrio, J.; Carretero, J. C. J. *Org. Chem.* **2006**, *71*, 5023. (k) Fructos, M. R.; Belderrain, T. R.; de Frémont, P.; Scott, N. M.; Nolan, S. P.; Díaz-Requejo, M. M.; Pérez, P. J. *Angew. Chem., Int. Ed.* **2005**, *44*, 5284. (l) Zhang, L.; Wang, S. J. *Am. Chem. Soc.* **2006**, *128*, 1442. (m) LaLonde, R. L.; Sherry, B. D.; Kang, E. J.; Toste, F. D. *J. Am. Chem. Soc.* **2006**, *129*, 2452. (n) Mézailles, N.; Ricard, L.; Gagosz, F. *Org. Lett.* **2005**, *7*, 4133. (o) Roembke, P.; Schmidbaur, H.; Cronje, S.; Raubenheimer, H. J. *Mol. Catal. A* **2004**, *212*, 35. (p) Barluenga, J.; Diéguez, A.; Fernández, A.; Rodríguez, F.; Fanañás, F. J. *Angew. Chem., Int. Ed.* **2006**, *45*, 2091.

- (3) (a) Hashmi, A. S. K.; Rudolph, M.; Weyrauch, J. P.; Woelfle, M.; Frey, W.; Bats, J. W. *Angew. Chem.* **2005**, *117*, 2858. (b) Hashmi, A. S. K. *Gold Bull.* **2003**, *36*, 3.
- (4) (a) Nieto-Oberhuber, C.; López, S.; Muñoz, M. P.; Buñuel, E.; Nevado, C.; Cárdenas, D. J.; Echavarren, A. M. *Angew. Chem., Int. Ed.* **2004**, *43*, 2402. (b) Nevado, C.; Echavarren, A. M. *Chem. Eur. J.* **2005**, *11*, 3155. (c) Nieto-Oberhuber, C.; López, S.; Muñoz, M. P.; Jimenez-Núñez, E.; Buñuel, E.; Cárdenas, D. J.; Echavarren, A. M. *Chem. Eur. J.* **2006**, *12*, 1694.
- (5) (a) Shi, Z.; He, C. J. *Org. Chem.* **2004**, *69*, 3669. (b) Shi, Z.; He, C. J. *Am. Chem. Soc.* **2004**, *126*, 5964.
- (6) (a) Arcadi, A.; Bianchi, G.; Marinelli, F. *Synthesis* **2004**, 610. (b) Mamane, V.; Gress, T.; Krause, H.; Fürstner, A. J. *Am. Chem. Soc.* **2004**, *126*, 8654. (c) Sherry, B. D.; Toste, F. D. *J. Am. Chem. Soc.* **2004**, *126*, 15978. (d) Yao, T.; Zhang, X.; Larock, R. C. *J. Am. Chem. Soc.* **2004**, *126*, 11164. (e) Zhang, L.; Kozmin, S. A. *J. Am. Chem. Soc.* **2004**, *126*, 11806. (f) Guan, B.; Xing, D.; Cai, G.; Wan, X.; Yu, N.; Fang, Z.; Yang, L.; Shi, Z. *J. Am. Chem. Soc.* **2005**, *127*, 18004. (g) Asao, N.; Aikawa, H.; Yamamoto, Y. *J. Am. Chem. Soc.* **2004**, *126*, 7548. (h) Nguyen, R.-V.; Yao, X.-Q.; Bohle, D. S.; Li, C.-J. *Org. Lett.* **2005**, *7*, 673. (i) Georgy, M.; Boucard, V.; Campagne, J.-M. *J. Am. Chem. Soc.* **2005**, *127*, 14180. (j) Sromek, A. W.; Rubina, M.; Gevorgyan, V. *J. Am. Chem. Soc.* **2005**, *127*, 10500. (k) Antonioti, S.; Genin, E.; Michelet, V.; Genêt, J. *J. Am. Chem. Soc.* **2005**, *127*, 9976.
- (7) (a) Quian, H.; Han, X.; Widenhoefer, R. A. *J. Am. Chem. Soc.* **2004**, *126*, 9536. (b) Bender, C. F.; Widenhoefer, R. A. *J. Am. Chem. Soc.* **2005**, *127*, 1070.
- (8) Oe, Y.; Ohta, T.; Ito, Y. *Chem. Commun.* **2004**, 1620.
- (9) (a) Stahl, S. S. *Angew. Chem., Int. Ed.* **2004**, *43*, 3400. (b) Kawatsura, M.; Hartwig, J. F. *J. Am. Chem. Soc.* **2000**, *122*, 9546. (c) Utsunomiya, M.; Hartwig, J. F. *J. Am. Chem. Soc.* **2003**, *125*, 14286.

Scheme 1. Schematic Representation of the Studied Reaction: Hydroamination of 1,3-Dienes by CbzNH_2



the reactions catalyzed by gold, hydroamination of C—C multiple bonds (alkynes,¹⁰ alkenes,^{11–16} and allenes¹⁷) has received considerable attention for the synthesis of amine derivatives.¹⁸ Concerning the hydroamination of alkenes, He and co-workers reported that N-nucleophiles¹¹ (as well as O-nucleophiles)¹² can take part in nucleophilic additions with inert olefins or allenes. The study was extended to develop an efficient method for the hydroamination of 1,3-dienes to produce allylic amines.¹³ Simultaneously with the aforementioned work, Widenhoefer's group reported the intramolecular hydroamination of isolated alkenes.¹⁴ In all these cases a gold(I) complex (based on a Au^{I} –phosphine structure) was used as catalyst to activate the unsaturated bonds. In a parallel work by the groups of He and Hartwig it was shown that triflic acid and metal triflates give similar results for the addition of amines (and alcohols) to alkenes.¹⁵

Despite all this work on the hydroamination of alkenes, a clear picture of the overall reaction mechanism is not available. On the basis of experimental observations, a general mechanism for this process was proposed, consisting on the following steps:¹³ the generation of the active species R_3PAuOTf from R_3PAuCl and AgOTf , which complex can coordinate the diene, the coordination of the diene is followed by the nucleophile attack of the N-nucleophile, and the reaction is completed by proton transfer from the amino group to the other carbon atom of the double bond, therefore forming the final product. A detailed knowledge of the proton-transfer step, which is a fundamental step common in nucleophilic additions, however, remains elusive. With this aim, we present the computational investigation of the complete reaction mechanism for the hydroamination of conjugated alkenes, paying special attention to the hydrogen-transfer step.

In the present work, we tried to provide a theoretical description for the reaction mechanism of the hydroamination alkenes catalyzed by R_3PAuOTf , and we selected 1,3-diene as alkene and benzyl carbamate (CbzNH_2) as N-nucleophile (Scheme 1). Theoretical calculations concerning the reaction mechanism of processes catalyzed by gold complexes are still rather scarce;¹⁹ hence, additional studies on gold-based catalysis are desirable to acquire deeper understanding of its reactivity.

Computational Details

Complex H_3PAuOTf was adopted as a model for the catalytically active Ph_3PAuOTf species (formed from R_3PAuCl), but in some cases the effect of this ligand simplification was tested by carrying out calculations with the real PPh_3 ligand. As far as the reactants are concerned, 3-methyl-1,3-pentadiene and benzyl carbamate (CbzNH_2) were used for the calculations.

Density functional theory calculations were carried out to identify the structures of the reaction intermediates and transition states of the catalytic process. This method is shown to be appropriate to describe gold-based systems.^{20,21} In the case of the transition states, normal coordinate analysis has been used to calculate the imaginary frequencies, and for each transition structure we calculated the intrinsic reaction coordinate (IRC) routes toward the corresponding minima. If the IRC calculations failed to reach the energy minima on the potential energy surface, we performed geometry optimizations from the final phase of the IRC path.

All DFT calculations used the program package Gaussian 03²² and the B3LYP²³ combination of functionals. The LANL2DZ²⁴ pseudo-potential was employed for the gold center, and the standard 6-31G(d) basis set was used for the other atoms.²⁵ The reliability of the used basis set was tested by performing single-point calculations on the optimized structures using LANL2DZ/6-311++G(d,p) basis set (see Supporting Information). For the obtained structures, we estimated the effect of the bulk medium considering dichloroethane (DCE) as the solvent by the application of the polarizable continuum model (PCM)²⁶ as implemented in Gaussian 03; $\epsilon(\text{DCE}) = 10.4$. All energies given in the text correspond to the energy including the effect of the bulk solvent, which was obtained by adding the contribution of the Gibbs energy of solvation to the gas-phase total energies. For some particular steps (indicated in the text) the geometries and energies were obtained by reoptimizing the structures including solvent effects by means of the PCM method.

Results

The results are presented in several sections, each one devoted to a main step within the reaction mechanism. The first section analyzes the formation of the active gold catalytic species. The second section considers the substrate coordination to the catalytic center, whereas the next section is devoted to the nucleophilic attack of the carbamate substrate to the alkene. The last section examines several alternatives for the proton-transfer process between the amino group and the double bond.

Formation of the Active Catalyst. The first step of the reaction is the substitution of the chloride by a triflate ligand in the precursor Ph_3PAuCl complex to form the active species Ph_3PAuOTf . Experimental works show that the catalytic activities

- (10) Some examples: (a) Hashmi, A. S. K.; Rudolph, M.; Schymura, S.; Visus, J.; Frey, W. *Eur. J. Org. Chem.* **2006**, 4634. (b) Kadzimirsz, D.; Hildebrandt, D.; Merz, K.; Dyker, G. *Chem. Commun.* **2006**, 661. (c) Grin, D. J.; Davis, N. R.; Toste, F. D. *J. Am. Chem. Soc.* **2005**, 127, 11260.
 (11) Zhang, J.; Yang, C-G.; He, C. *J. Am. Chem. Soc.* **2006**, 128, 1798.
 (12) Yang, C-G.; He, C. *J. Am. Chem. Soc.* **2005**, 127, 6966.
 (13) Brouwer, C.; He, C. *Angew. Chem., Int. Ed.* **2006**, 45, 1744.
 (14) (a) Han, X.; Widenhoefer, R. A. *Angew. Chem., Int. Ed.* **2006**, 45, 1747. (b) Bender, D. F.; Widenhoefer, R. A. *Chem. Commun.* **2006**, 4143. (c) Bender, D. F.; Widenhoefer, R. A. *Org. Lett.* **2006**, 8, 5303.
 (15) (a) Li, Z.; Zhang, J.; Brouwer, C.; Yang, C-G.; Reich, N. W.; He, C. *Org. Lett.* **2006**, 8, 4174. (b) Rosenfeld, D. C.; Shekhar, S.; Takemiya, A.; Utsunomiya, M.; Hartwig, J. F. *Org. Lett.* **2006**, 8, 4179.
 (16) Liu, X.-Y.; Li, D.-H.; Che, C.-M. *Org. Lett.* **2006**, 8, 2707.
 (17) Some examples: (a) Nishina, N.; Yamamoto, Y. *Angew. Chem., Int. Ed.* **2006**, 45, 3314. (b) Morita, N.; Krause, N. *Eur. J. Org. Chem.* **2006**, 4634. (c) Zhang, Z.; Liu, C.; Kinder, R. E.; Han, X.; Qian, H.; Widenhoefer, R. A. *J. Am. Chem. Soc.* **2006**, 128, 9066.
 (18) Widenhoefer, R. A.; Han, X. *Eur. J. Org. Chem.* **2006**, 4555.

- (19) Some examples: (a) Comas-Vives, A.; Gonzalez-Arellano, C.; Corma, A.; Iglesias, M.; Sanchez, F.; Ujaque, G. *J. Am. Chem. Soc.* **2006**, 128, 4756. (b) Faza, O. N.; López, C. S.; Alvarez, R.; de Lera, A. R. *J. Am. Chem. Soc.* **2006**, 128, 2434. (c) Soriano, E.; Marco-Contelles, J. *Organometallics* **2006**, 25, 4542. (d) Nevado, C.; Echavarren, A. M. *Chem. Eur. J.* **2005**, 11, 3155. (e) Straub, B.F. *Chem. Commun.* **2004**, 1726.
 (20) An excellent review on theoretical treatment of gold: Pykkö, P. *Angew. Chem., Int. Ed.* **2004**, 43, 4412.
 (21) Gorin, D. J.; Toste, F. D. *Nature* **2007**, 446, 395.
 (22) Frisch, M. J.; et al. *Gaussian 03*, revision C.02; Gaussian, Inc.: Pittsburgh, PA, 2004.
 (23) (a) Becke, A. D. *J. Chem. Phys.* **1993**, 98, 5648. (b) Lee, C.; Yang, W.; Parr, R. G. *Phys. Rev. B.* **1988**, 37, 785. (c) Stephens, P. J.; Devlin, F. J.; Chabalowski, C. F.; Frisch, M. J. *J. Phys. Chem.* **1994**, 98, 11623.
 (24) (a) Hay, P. J.; Wadt, W. R. *J. Chem. Phys.* **1985**, 82, 270. (b) Wadt, W. R.; Hay, P. J. *J. Chem. Phys.* **1985**, 82, 284. (c) Hay, P. J.; Wadt, W. R. *J. Chem. Phys.* **1985**, 82, 299.
 (25) (a) Hariharan, P. C.; Pople, J. A. *Mol. Phys.* **1974**, 27, 209. (b) Rassolov, V. A.; Ratner, M. A.; Pople, J. A.; Redfern, P. C.; Curtiss, L. A. *J. Comput. Chem.* **2001**, 22, 976.
 (26) (a) Miertus, S.; Scrocco, E.; Tomasi, J. *J. Chem. Phys.* **1981**, 55, 117. (b) Barone, V.; Cossi, M.; Tomasi, J. *J. Chem. Phys.* **1997**, 107, 3210.

Table 1. Relative Metal–Ligand (PAu–X) Dissociation Energies in Dichloroethane (DCE)

| P X | OTf ^{−a} | NO ₃ [−] | Cl [−] | TsO [−] | CF ₃ COO [−] | BF ₄ [−] |
|------------------|-------------------|------------------------------|-----------------|------------------|----------------------------------|------------------------------|
| PH ₃ | 0.0 | 11.0 | 12.3 | 7.1 | 13.0 | −4.3 |
| PPh ₃ | 0.0 | 8.2 | 12.5 | 6.3 | 13.2 | −2.3 |

^a The calculated reaction energy for the dissociation process in DCE is 29.9 kcal/mol with PH₃ and 24.6 kcal/mol with PPh₃ ligands.

are quite different, depending on the counterions present in the active gold species.¹³ The catalyst was prepared from Ph₃PAuCl and silver salts of different anions. OTf[−], NO₃[−] and CF₃COO[−] were not proved to be efficient as counterions, probably since they form strong interaction with the gold metal center; anions such as BF₄[−] or OTf[−], however, were good for the reaction. The experiments also showed that coordinating solvents such as 1,4-dioxane or nitromethane decreased the catalytic activity, whereas noncoordinating solvents such as dichloroethane (DCE) have not caused such problems.¹³ To analyze what is the effect of the ligand (counterion) on the reaction mechanism we calculated the bonding energies in dichloroethane between PH₃Au⁺ and different anions used in the experiment (eq 1).



(P = PH₃ or PPh₃, whereas X = Cl, NO₃, OTf, TsO, CF₃COO, BF₄).

In Table 1 the relative energies for the reaction depicted in eq 1 are shown. For the sake of comparison the energy reaction PAuOTf → PAu⁺ + OTf[−] is defined as zero. It can be seen that the interaction between triflate or BF₄[−] and the gold center is much weaker than that of gold(I) and chloride, nitrate, tosylate, or trifluoromethyl-acetate anions, which is consistent with the experimental results. As expected, OTf[−] and BF₄[−] are better leaving groups than the other counterions shown in the table. Therefore, substitution of the chloride ligand by triflate or BF₄[−] facilitates the ligand substitution process for the coordination of the diene; conversely, the combination of PAuOTf with AgNO₃, AgOTs, or AgOOCF₃ does not lead to reaction, since these latter anions also interact strongly with the gold center and do not facilitate their substitution by diene. Results in Table 1 also show that the effects of using the real PPh₃ ligands instead of PH₃ are rather small in terms of comparing the different counterions.

In the experimental work Ph₃PAuOTf was proposed as the catalytically active species, which is formed by mixing Ph₃PAuCl and AgOTf in anhydrous dichloroethane. Formation of Ph₃PAuOTf from Ph₃PAuCl and AgOTf is unfavorable, as it is shown by the bonding energy values in Table 1; however, precipitation of AgCl from the solution leads to stoichiometric formation of the catalytically active species. This species is considered as the active species involved in the catalytic cycle.

First Step: Diene Coordination. Once the gold active species is formed, the next step should correspond to the ligand substitution, OTf[−] by the alkene. The initial coordination of the CbzNH₂ to the gold complex was not experimentally observed by analyzing the ³¹P NMR signal when mixing the nucleophile with the catalyst.¹³ The formation of [H₃PAu(CbzNH₂)]⁺ in the reaction between H₃PAuOTf and CbzNH₂ is characterized by a reaction energy of 12.2 kcal/mol. In addition, the formation of H₃PAu(CbzNH) and HOTf species

was also considered (due to the fact that triflic acid was found to catalyze the reaction),¹⁵ but this process is even more unfeasible thermodynamically (18.2 kcal/mol), compared to the initial coordination of the diene (vide infra). Therefore, a pathway with the initial coordination of CbzNH₂ to the gold catalyst can be discarded.

The diene may coordinate to the metal center in several ways: through both double bonds simultaneously or through one of the double bonds. Calculations showed that the most stable coordination of the diene is through only one of the double bonds as depicted in Figure 1, structure 2, maintaining a linear arrangement. The coordination of the diene via both double bonds and forming a tricoordinate square planar structure seems unfavorable on the basis of the calculations; a minimum of this type was not possible to locate on the potential energy surface.²⁷

The optimized structure after ligand substitution, 2, can be also described as a linear gold complex (see Figure 1). The energy change for the triflate by diene ligand substitution is −4.8 kcal/mol. Once the olefin is coordinated, it is activated (the C–C distance is 1.338 Å in the free diene and 1.384 Å, when coordinated) to undertake the nucleophilic addition.

Second Step: Nucleophile Attack to the C–C Double Bond. The coordination of the diene to the metal center facilitates the nucleophilic attack. In a previous study on a related system, Teles et al. proposed a mechanism for the nucleophilic attack of methanol to propyne catalyzed by trimethylphosphane–gold(I).²⁸ In that case, the O-nucleophile was coordinated to the metal center previous to the nucleophilic attack. We checked the same possibility for the N-nucleophile, but calculations show that the N-nucleophile (CbzNH₂) does not coordinate to the gold center. Optimization of a 3-coordinated structures adding the amino group to the metal center was unsuccessful, always ending up in two-coordinated structures as 3. Benzyl carbamate forms weak interaction with the metal center through one of its oxygen atoms (*d*(Au–O) = 3.163 Å, see Figure 2). This is consistent with the experimental results where no spectroscopically detectable interaction was found between the metal center and the nucleophile.¹³ Therefore, the mechanism of the nucleophilic attack of N-nucleophiles on alkenes catalyzed by gold(I), according to these calculations, does not imply a coordination of the N-nucleophile. We have to mention, however, that the addition of N- and O-nucleophiles using gold catalyst can proceed through different reaction mechanisms.

At this point the system is ready to start the hydroamination process properly speaking. Several pathways are considered here for the nucleophilic attack. The N-nucleophile can attack the double bond from the side of the metal center (metal-side) or from the outside of the complex (bulk-side); see Scheme 2. Calculations show that attack from the outside proceeds through much lower barriers; the attack from the side of the metal center to form the Markovnikov product proceeds through a barrier 7.2 kcal/mol higher than for the attack from outside. The structures and energy data for the metal-side mechanism can be found in the Supporting Information. These results are in concordance with the stereochemical analysis of the intramo-

(27) A study on the coordination mode of d¹⁰ metal centers: Carvajal, M. A.; Novoa, J. J.; Alvarez, S. *J. Am. Chem. Soc.* **2004**, *126*, 1465.

(28) Teles, J. H.; Brode, S.; Chabanas, M. *Angew. Chem.* **1998**, *110*, 1475.

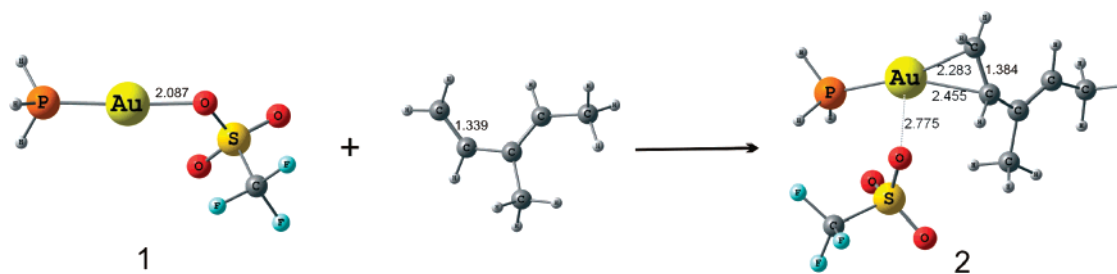


Figure 1. Coordination of 3-methyl-1,3-pentadiene to the catalytically active species H_3PAuOTf .

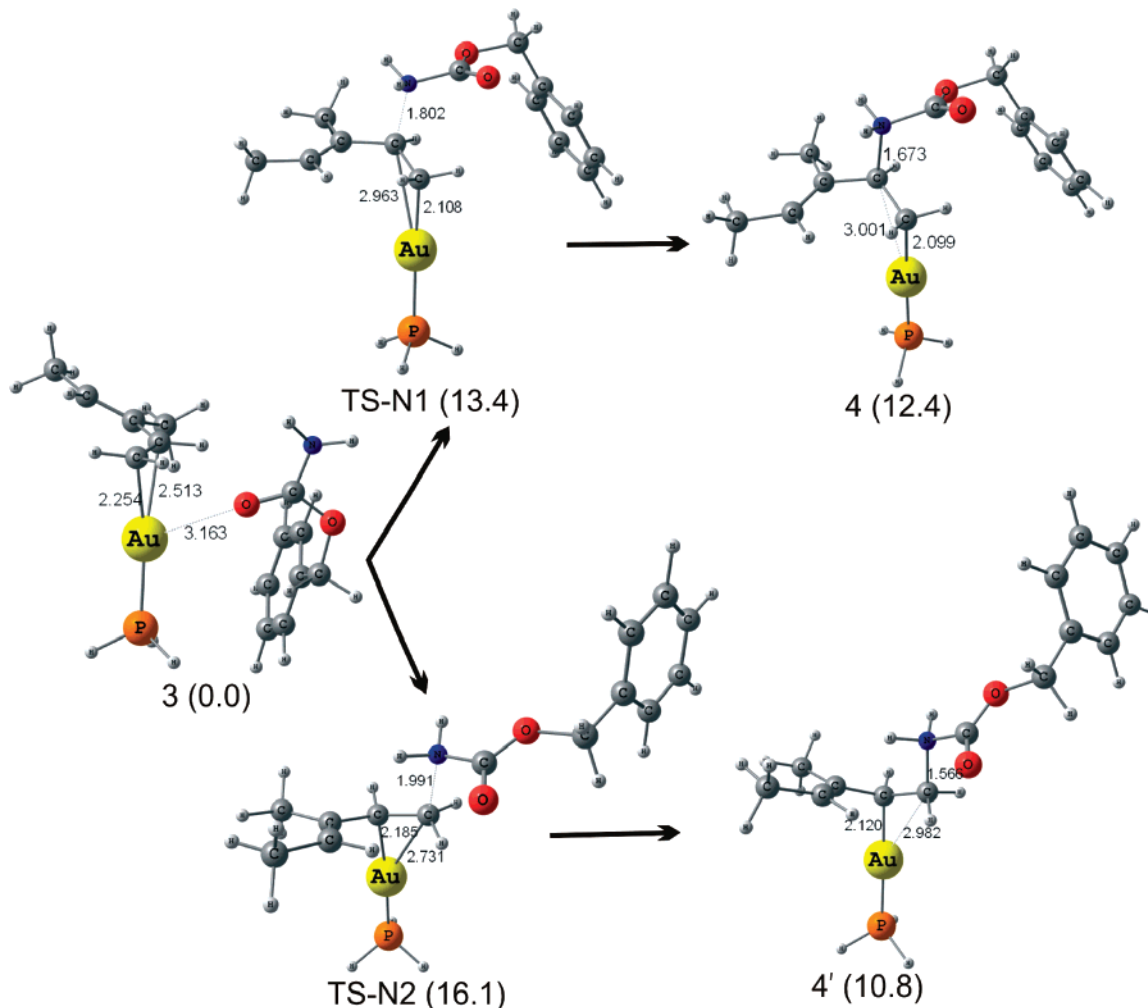
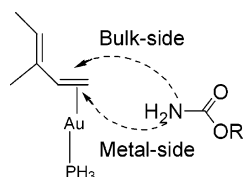


Figure 2. Nucleophile attack of CbzNH_2 on the gold-coordinated 3-methyl-1,3-pentadiene. Energies in parentheses (kcal/mol).

Scheme 2. Schematic Representation of the Metal- and Bulk-Side Attack of the N-Nucleophile on the Coordinated Double Bond



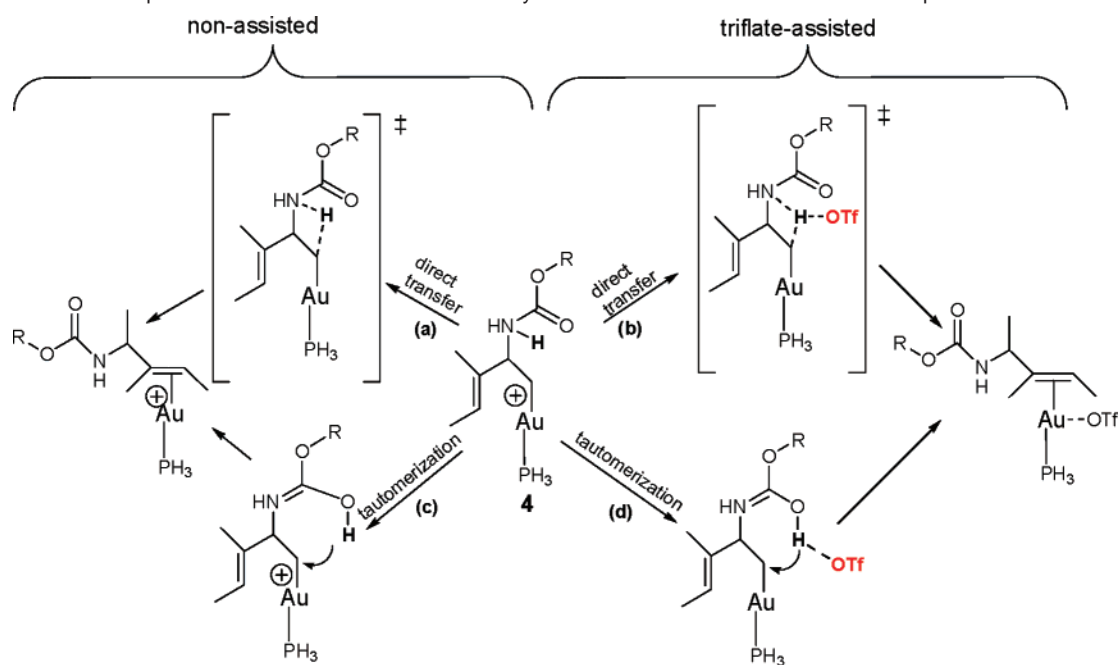
lecular addition of alcohols to alkynes where a bulk-side mechanism is supported.^{29,30} In Figure 2 the structures for the bulk-side mechanism are presented: **TS-N1** represents the transition state, which leads to the Markovnikov product (**4**),

whereas **TS-N2** leads the reaction to the Anti-Markovnikov product (**4'**). In both transition states, the bond between the gold center and the carbon atom, on which the nucleophile attacks, is elongated, while the other Au–C distance becomes shortened. The calculated energy barriers favor the formation of the detected (Markovnikov) product by 2.7 kcal/mol, in agreement with experiments.

Third Step: Proton-Transfer between the Amine Group and the Olefin. The most intricate and unexplored part of the reaction mechanism corresponds to the proton transfer from the N-atom to the C-atom of the activated double bond. This proper step cannot be easily analyzed in detail by experimental works. Schwarz and co-workers observed experimentally that nucleophilic addition of alcohols to alkynes does not proceed in the gas phase, thus suggesting that solvent (MeOH)-assisted hy-

(29) Kennedy-Smith, J. J.; Staben, S. T.; Toste, F. D. *J. Am. Chem. Soc.* **2004**, *126*, 4526.

(30) Liu, Y.; Song, F.; Song, Z.; Liu, M.; Yan, B. *Org. Lett.* **2005**, *7*, 5409.

Scheme 3. Schematic Representation of the Mechanistic Pathways Considered for the Proton-Transfer Step

drogen migration might be crucial for the reaction.³¹ In the currently presented case, dichloroethane was used as solvent, which assumes solvent participation being unlikely. Nevertheless, proton-transfer reactions have been shown to be assisted by the presence of anionic species^{32–36} or neutral bases,³⁷ and we decided to check this possibility.

In our analysis, four possible mechanistic pathways were considered for the proton-transfer step. In two of them the proton transfer is assisted by a triflate anion (generated in the first step of the reaction), whereas in the other two pathways the proton transfer is not assisted (see Scheme 3). The four considered pathways are the following:

- direct proton transfer from the nitrogen to the carbon,
- triflate-assisted direct proton transfer from nitrogen to carbon,
- CbzNH₂ tautomerization followed by transfer of the proton from the O–H group of the tautomer to the carbon atom,
- CbzNH₂ tautomerization and transfer of the proton from the O–H group of the tautomer to the carbon atom assisted by triflate anions.

(a) Direct Proton Transfer from the NH₂ Group to the Carbon Atom. One possibility for the completion of the reduction is that one of the hydrogens from the NH₂ group is directly transferred to the unsaturated carbon atom. The direct proton-transfer process was investigated for both the Markovnikov and anti-Markovnikov addition; in Figure 3, however,

only the stationary points giving the Markovnikov intermediate are shown. In the transition states, **TS-PT1** and **TS-PT2**, the transferred proton is forming a C–NH four-membered ring, which accounts for the calculated high barriers. The proton transfer leads to the rupture of the Au–C bond, and optimization leads to **5** and **5'** intermediates, in which the product is coordinated to the metal center via the other C–C double bond.

The calculated barriers for the direct transfer of the hydrogen to the carbon are 39.4 kcal/mol for the formation of the Markovnikov product, and 46.2 kcal/mol for the anti-Markovnikov product. This shows that the proton transfer in the case of the experimentally obtained product is favored by 6.8 kcal/mol. Nevertheless, these barriers are too high, thus this pathway can be ruled out and other pathways need to be considered. In the following alternative pathways, only the mechanistic description of the reactions that give rise to the experimentally detected product (Markovnikov) were considered.

(b) Triflate-Assisted Proton Transfer from Nitrogen to Carbon. The fact that anions can assist proton transfers lowering the energy barriers has been already shown in the literature for the case of heterolytic activation of C–H bonds. For instance, Eisenstein, Crabtree, and co-workers demonstrated that anions were able to assist the C–H heterolytic activation and proton transfer of the H to another ligand coordinated to the metal.³² Other separated studies by Macgregor,³³ Maseras,³⁴ and Basallote and Lledós groups,^{35,36} respectively, also revealed that anionic species can facilitate proton-transfer reactions. Moreover, it has also been shown that the presence of a neutral base can catalyze proton-transfer processes.³⁷

For this particular reaction we analyzed whether triflate anions have similar effects on the actual proton-transfer step. The optimized structures representing this pathway are shown in Figure 4. In structure **6** triflate anion forms hydrogen bonds with both of the N–H protons via the oxygens, whereas in the transition state **TS-PT2a**, the transferred proton is found between the triflate oxygen and the nitrogen atom. In the intermediate

- Roithova, J.; Hrusak, J.; Schroder, D.; Schwarz, R. *Inorg. Chim. Acta* **2005**, *358*, 4287.
- Appelhans, L. N.; Zuccaccia, D.; Kovacevic, A.; Chianese, A. R.; Miecznikowski, J. R.; Macchioni, A.; Clot, E.; Eisenstein, O.; Crabtree, R. H. *J. Am. Chem. Soc.* **2005**, *127*, 16299.
- Davies, D. L.; Donald, S. M. A.; Macgregor, S. A. *J. Am. Chem. Soc.* **2005**, *127*, 13754.
- García-Cuadrado, D.; Braga, A. A. C.; Maseras, F.; Echavarren, A. M. *J. Am. Chem. Soc.* **2006**, *128*, 1066.
- Basallote, M. G.; Besora, M.; Duran, J.; Fernández-Trujillo, M. J.; Lledós, A.; Máñez, M. A.; Maseras, F. *J. Am. Chem. Soc.* **2004**, *126*, 2320.
- Basallote, M. G.; Besora, M.; Castillo, C. E.; Fernández-Trujillo, M. J.; Lledós, A.; Maseras, F.; Máñez, M. A. *J. Am. Chem. Soc.* **2007**, *129*, 6608.
- Balcells, D.; Ujaque, G.; Fernandez, I.; Khar, N.; Maseras, F. *J. Org. Chem.* **2006**, *71*, 6388.

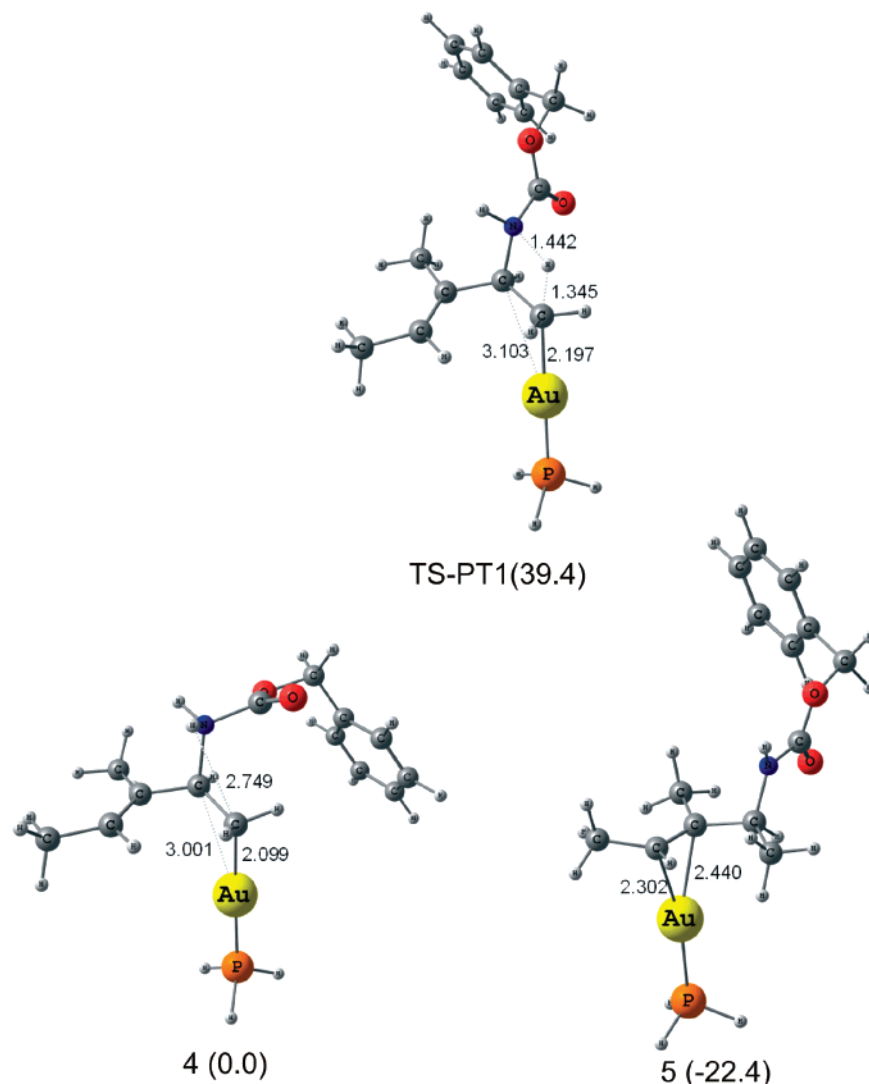


Figure 3. Intermediates and TS for the proton transfer from NH_2 to the unsaturated carbon atoms for the Markovnikov product. Energies in parentheses (kcal/mol).

7, the hydrogen is transferred to the triflate, and the subsequent transition state, **TS-PT2b**, corresponds to the proton transfer from the triflic acid to the unsaturated carbon atom. In the product, **8**, the Au–C is ruptured and the product stays coordinated via its remaining unsaturated double bond. If we consider the relative energies of the optimized stationary points, the proton transfer is more likely to proceed as a one-step reaction. Intermediate **7** represents a very flat minimum; the barrier for going back to intermediate **6** is characterized by an almost negligible 0.1 kcal/mol barrier. Similar results were obtained when these stationary points were calculated optimizing the geometries including solvent effects. In the latter case, the relative energies for **6**, **TS-PT2a**, **7**, **TS-PT2b**, and **8** are 0.0, 7.5, 7.3, 27.8, and -14.9 kcal/mol, respectively; the corresponding values for PCM single-point calculations on gas-phase geometries are 0.0, 6.7, 6.6, 26.6, and -15.0 kcal/mol, respectively (Figure 4). Despite the great effort devoted, a transition state for the single direct proton transfer assisted by a triflate was not located.

The overall barrier for this proton-transfer process is 26.6 kcal/mol, which corresponds to the highest energy barrier. This mechanistic pathway represents a more favorable pathway than the direct proton transfer from the nitrogen to the carbon (26.6

vs 39.4 kcal/mol). This result shows that the presence of triflate is able to catalyze the N–H heterolytic bond splitting. Although the process through this energy barrier seems feasible, we investigated other reasonable reaction pathways.

(c) CbzNH_2 Tautomerization and Transfer of the Proton from the O–H Group of the Tautomer to the Carbon Atom.

Another possible reaction mechanism for the proton transfer involves the tautomerization of the carbamate moiety from the “ $\text{H}_2\text{N}-\text{C}=\text{O}$ ” to the “ $\text{HN}=\text{C}-\text{OH}$ ” form, with the subsequent proton transfer from the O–H group to the carbon atom to complete the reaction. The tautomer forms of benzyl carbamate are shown in Scheme 4.

This whole process was considered first without the participation of triflate anions, that is, the direct tautomerization of carbamate moiety, which is shown in Figure 5. This process is characterized by a four-membered COHN-ring transition state (**TS-Tau1**). This process has a very high-energy barrier (45.2 kcal/mol). The relative energy between the two tautomeric forms, 1.7 kcal/mol, however, is rather low. We also considered the tautomerization of the free substrate (benzyl carbamate), but the calculations showed that the “ $\text{H}_2\text{N}-\text{C}=\text{O}$ ” form is considerably more stable in energy (by 12.7 kcal/mol) than the “ $\text{HN}=\text{C}-\text{OH}$ ” form, which shows the tautomerization of the free

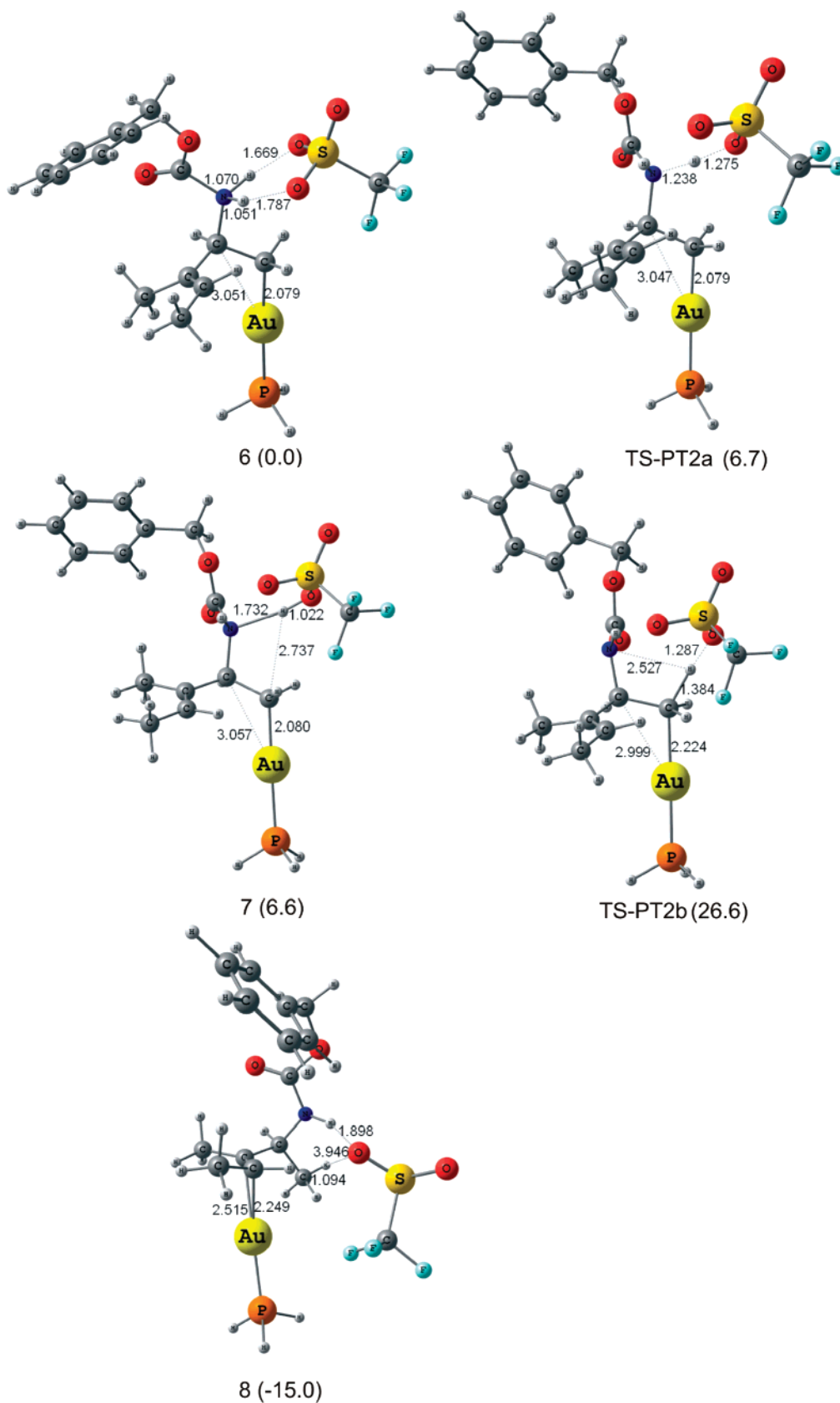
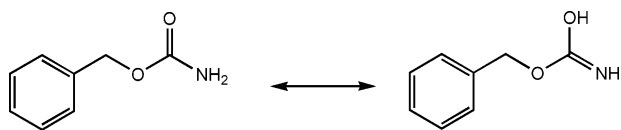


Figure 4. Optimized geometries for the pathway involving the proton transfer assisted by triflate. Energies in parentheses (kcal/mol).

substrate, as expected, is an unlikely process. Nevertheless, once the nucleophile is added to the alkene, the tautomers are nearly thermoneutral. The same happens in both situations, when the nucleophile is added to the bonded or to the dangling double

bond, therefore indicating that the metal center does not directly contribute to the thermoneutrality. The tautomerization energy is mainly affected by the fact of having the CbzNH₂ added to the alkene. To confirm this assumption, calculations were carried

Scheme 4. Tautomer Forms of Benzyl Carbamate

out without the metal center, by substituting the “H₃PAu-” groups by a hydrogen. The energy difference between the two tautomers was found to be 0.8 kcal/mol, thus showing that thermoneutrality between both tautomers is due to the fact that the N-nucleophile is bonded to the double bond, and the Au center does not have a direct role on this.

After the tautomerization, the proton from the “OH” group can be transferred to the carbon to complete the hydroamination reaction. In the transition state **TS-PT3**, the hydrogen lies between the oxygen and the carbon atoms with distances of $d(\text{O}-\text{H}) = 1.342 \text{ \AA}$ and $d(\text{N}-\text{H}) = 1.300 \text{ \AA}$, respectively. This latter process is characterized by a rather low barrier (14.0 kcal/mol); however, the rate-determining step would be the first one, which is characterized by a very high barrier. Through the tautomerization, the barrier for the proton transfer to the carbon atom step has been notably reduced. However, the barrier for the tautomerization is too high to make this mechanism feasible. This mechanism represents an energetically unfavorable pathway; thus, the alternative mechanism including the OTf⁻-assisted tautomerization was also evaluated.

(d) CbzNH₂ Tautomerization and Transfer of the Proton from the O–H Group of the Tautomer to the Carbon Atom Assisted by Triflate Anions. Since the experiments were taking place in dichloroethane, solvent-assisted tautomerization or any kind of solvent-assisted proton transfer seemed unlikely. However, to confirm this assumption, calculations for the tautomerization in the presence of an explicit solvent molecule (DCE) were carried out. The results showed that, although the barrier for the tautomerization was lowered (38.5 kcal/mol) in comparison with the unassisted tautomerization (45.2 kcal/mol), this barrier is still quite high; thus, the assistance of the solvent in this reaction can be ruled out.

The transition state (**TS-Tau2**) corresponding to the triflate-assisted proton transfer from the nitrogen to the carboxyl oxygen (the tautomerization process) was optimized, and the geometry shows that the proton is mainly attached to the triflate oxygen $d(\text{O}-\text{H})_{\text{OTf}} = 0.986 \text{ \AA}$, while the $d(\text{N}-\text{H}) = 2.237 \text{ \AA}$ and $d(\text{O}-\text{H}) = 2.338 \text{ \AA}$ values are rather long (see Figure 6). In spite of this, the calculated imaginary frequency and the IRC calculations clearly indicated that this transition state corresponds to the aforementioned tautomerization process. The transition state clearly shows that the triflate accommodates the proton during the transfer process, serving as a proton shuttle in the reaction step.³⁸

The calculations showed that this pathway (Figure 6) can be characterized by a much lower barrier (9.7 kcal/mol) than that of the direct tautomerization (45.2 kcal/mol), indicating the important role of triflate ions in this reaction step. The energy difference between the two tautomers, intermediates **4** and **9'** is -1.6 kcal/mol . The fact that anions and bases can reduce dramatically the energy barriers of tautomerization processes is already known in the literature,³⁹ and our work demonstrates that triflate anions can play this role in this reaction.

(38) The hydroamination process was found to be also catalyzed by triflic acid (ref 15). Computational evaluation is under progress.

The presence of water impurities is inevitable even in absolute solvents; hence, the possible participation of water molecules in the tautomerization process was investigated. A transition state for the water-assisted tautomerization was obtained, with an energy barrier of 19.4 kcal/mol; the water molecule is here acting as a proton-donor/proton-acceptor species, instead of as a proton shuttle (the barrier in the latter case is 30.4 kcal/mol). The moderate energy barrier for this step, although significantly higher than in the case of triflate (9.7 vs 19.4 kcal/mol), may suggest the potential participation of water molecules in the reaction pathway. On the other side, on the basis of all these results one cannot exclude the participation of the basic surface of the reaction vessel (glass, with concentration of basic sites probably as high as the catalytic triflate ions in solution).⁴⁰

After the tautomerization, the proton from the OH group must be transferred to the unsaturated carbon atom. As it is shown in Figure 5, it can be transferred directly with a reasonably low (15.7 kcal/mol) barrier. This proton transfer in the presence of triflate anion was also examined. Calculation shows that the proton is initially transferred from the OH group to triflate along with a large structural reorganization ending up in a structure with a hydrogen bond between “triflic acid” and the amino group; the structure found was analogous to structure **7** (shown in Figure 4). Then, the product can be formed through **TS-PT2b**, which is characterized by a higher energy barrier (20.3 kcal/mol) than that of the direct proton transfer. Hence, the calculations suggest that in this process triflate only participates in the tautomerization step; conversely, the proton transfer from the “OH”-group is more favorable to take place directly.

Overall Reaction Mechanism. The energy profiles for the considered mechanistic pathways are shown in Figure 7. The reaction is considered to be initiated by the generation of the active species H₃PAuOTf. The presence of OTf⁻ ligand (compared to other anionic ligands) coordinated to the gold catalyst facilitates the coordination, and therefore the reactivity, of the alkenes. The N-nucleophile attacks the activated alkene, and the formation of the Markovnikov intermediate is energetically favored. The most striking part of the reaction mechanism is the H-transfer from the NH₂ group to the other carbon atom to complete the reaction mechanism. The direct H-transfer and the one going through an initial tautomerization process are both analyzed. In addition, the effect of the triflate anions assisting the proton transfer is also evaluated. Considering the energy profile, the most likely pathway is divided into two steps: (i) the triflate-assisted tautomerization of carbamate moiety from “H₂N–C=O” to the “HN=C–OH”, and (ii) the proton transfer from the newly formed OH group to the unsaturated carbon atom.

An important fact for the reaction is that the tautomerization process is facilitated when the N-nucleophile is added to the substrate. Hence, whereas the free CbzNH₂ does not tautomerize (energy difference between the tautomers is approximately 13.0 kcal/mol), once it is bonded to the olefin, the energy difference between the two tautomers is dramatically reduced to ca. 2 kcal/mol. In addition, the presence of OTf⁻ anions is crucial for the

(39) See for instance: (a) Lledós, A.; Bertran, J. *Tetrahedron Lett.* **1981**, 22, 775. (b) Ventura, O. N.; Lledós, A.; Bonaccorsi, R.; Bertran, J.; Tomasi J. *Theor. Chim. Acta* **1987**, 72, 175. (c) Chalk, A. J.; Radom, L. *J. Am. Chem. Soc.* **1997**, 119, 7573. (d) Simon, S.; Sodupe, M.; Bertran, J. *Theor. Chem. Acc.* **2004**, 111, 211. (e) Lima, M. C. P.; Coutinho, K.; Canuto, S.; Rocha, N. R. *J. Phys. Chem. A* **2006**, 110, 7253.

(40) We appreciate the reviewers' suggestions.

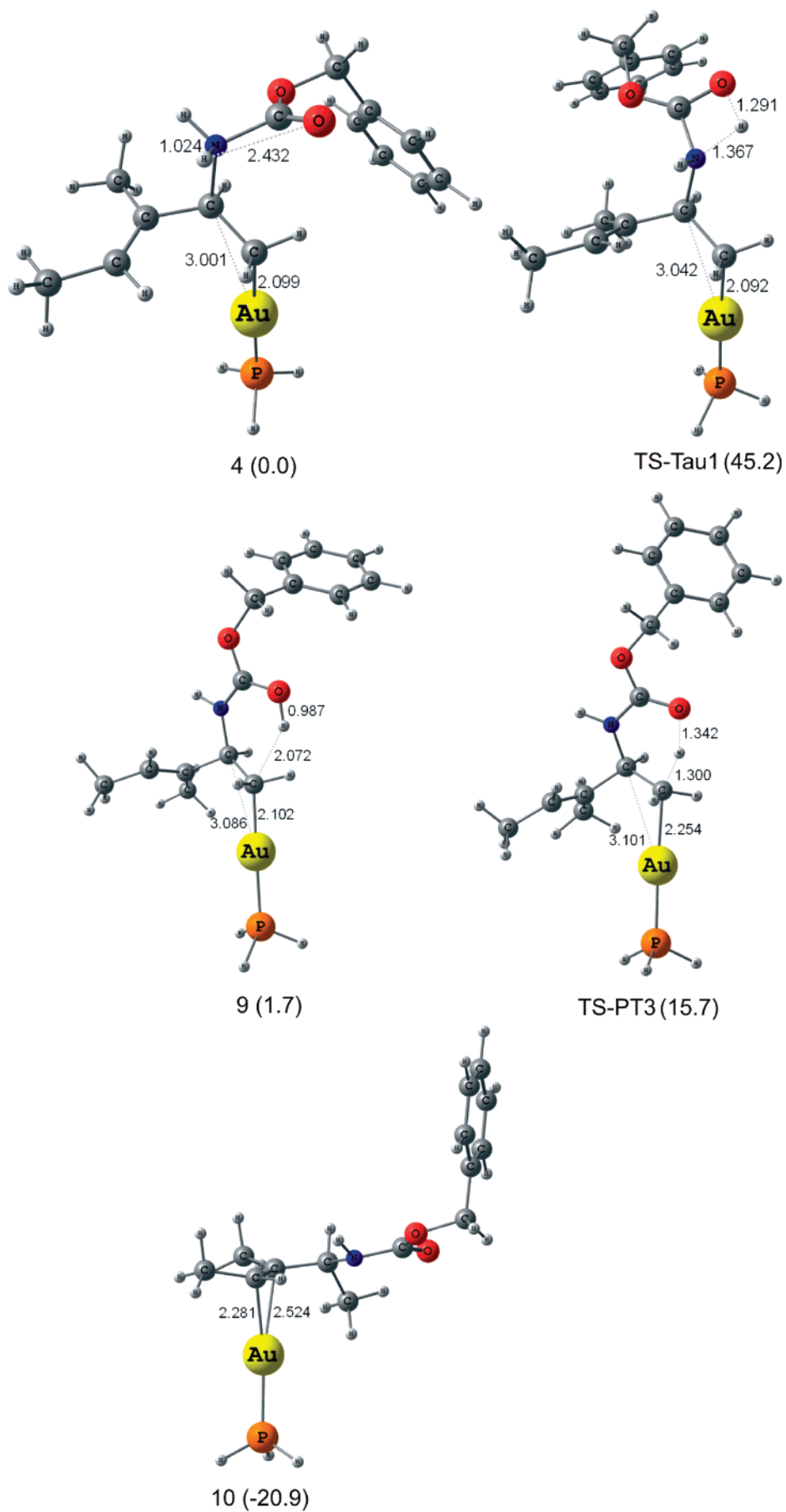


Figure 5. Optimized geometries for the direct tautomerization “ $\text{H}_2\text{N}-\text{C}=\text{O}$ ” \leftrightarrow “ $\text{HN}=\text{C}-\text{OH}$ ” process. Energies in parentheses (kcal/mol).

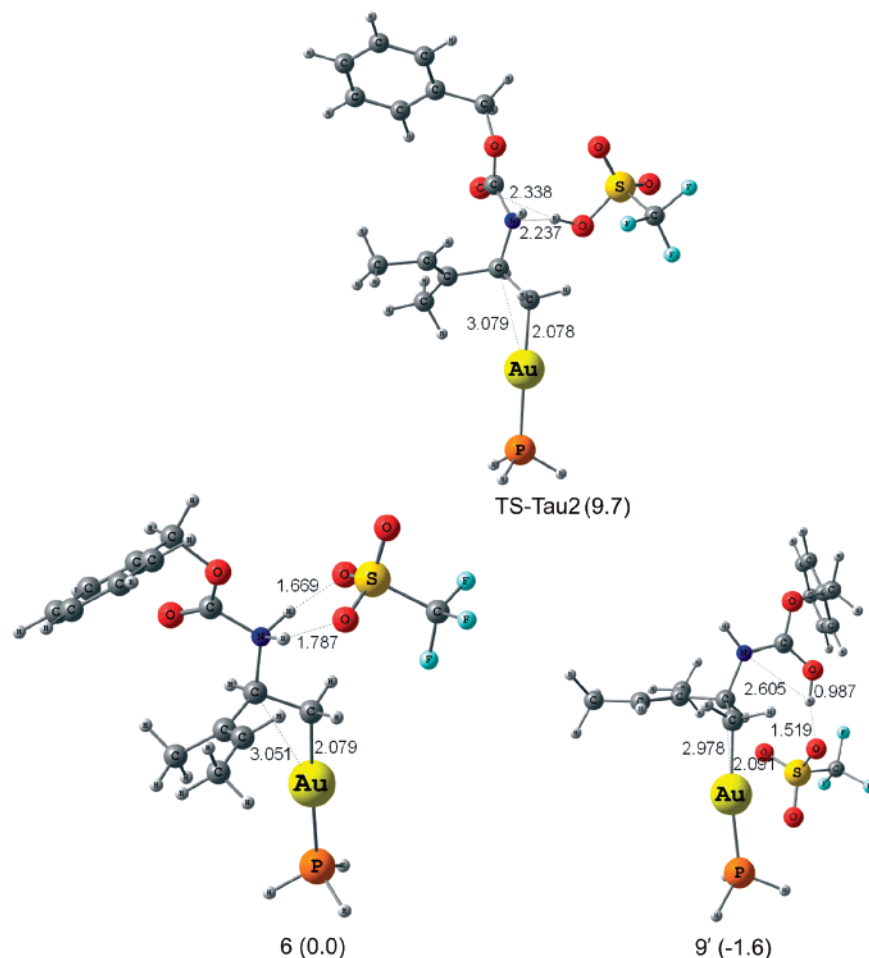


Figure 6. Optimized geometries for the triflate-assisted “NH₂-CO” ↔ “NH-CO(H)” tautomerization pathway. Energies in parentheses (kcal/mol).

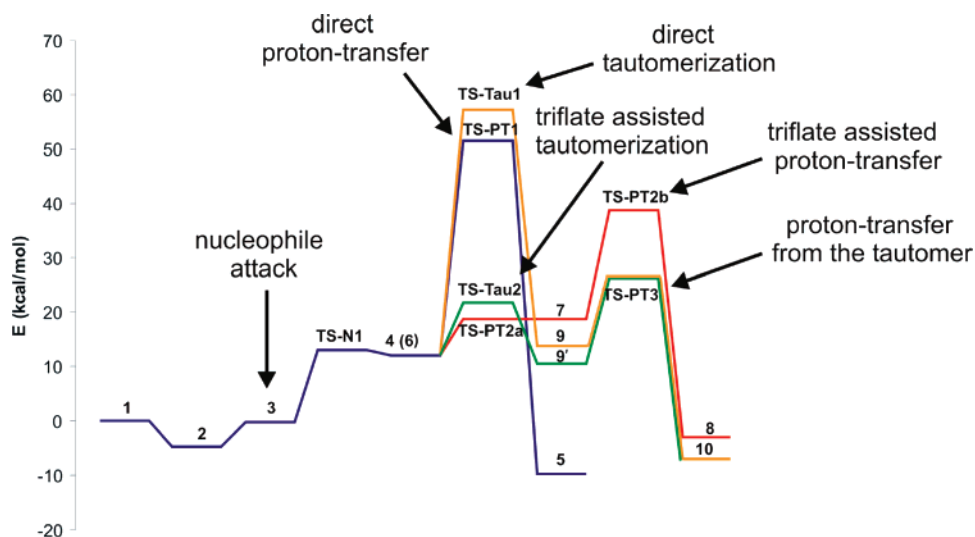
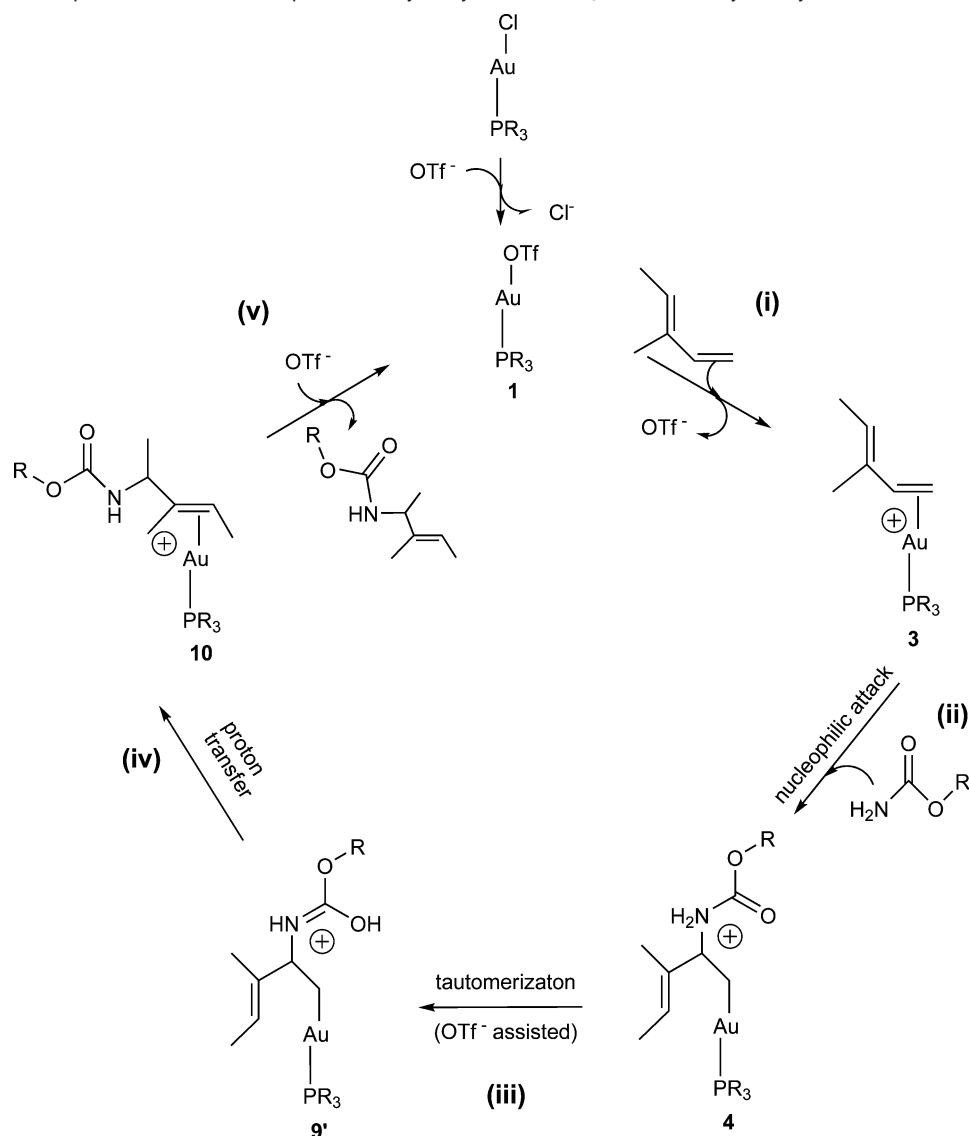


Figure 7. Energy profiles for the considered mechanistic pathways: (a) direct H-transfer, blue; (b) OTf⁻-assisted H-transfer, red; (c) tautomerization, orange; (d) OTf⁻-assisted tautomerization, green.

reaction since they highly diminish the reaction energy barrier for the tautomerization process, thus facilitating the overall reaction. Consequently, once CbzNH₂ is added to the alkene, the relative energy between tautomers is dramatically reduced, becoming near thermoneutral (thermodynamic effect), and the presence of triflate anions catalyze the interconversion process (kinetic effect).

Hydroamination using simple amines in the presence of gold complexes is not a generally described process in the literature. In fact, the N-nucleophiles utilized have protecting groups that are susceptible of undertaking a tautomeric process similar to the one here described.¹⁸ For instance, Morita and Krause⁴¹

(41) Morita, N.; Krause, N. *Org. Lett.* **2004**, *6*, 4121.

Scheme 5. Schematic Representation of the Proposed Catalytic Cycle for the $R_3PAuOTf$ -Catalyzed Hydroamination of Alkenes

found that gold-catalyzed cyclization reactions,⁴² which were based on N -nucleophilic addition steps, proceeded in several days in the case of free amino groups, whereas with sulfonamides as well as acetyl or Boc protecting groups fast conversion resulted. Hence, active participation of the protecting groups through the mechanism could explain these experiments.

Taking all these facts into consideration the catalytic cycle for the hydroamination of 1,3-dienes can be summarized as follows (Scheme 5): (i) OTf^- by alkene ligand substitution, (ii) nucleophilic attack to the activated alkene by the N -nucleophile, (iii) " $H_2N-C=O$ " \leftrightarrow " $HN=C-OH$ " tautomerization (OTf^- assisted), (iv) proton transfer, and (v) replacement of the product by OTf^- regenerating the catalyst species, therefore closing the catalytic cycle. This latter step can imply also the direct substitution of the reaction product by an initial reactant to keep going within the catalytic cycle.

Conclusion

Several mechanistic possibilities for the gold(I)–phosphine catalyzed hydroamination of 1,3-dienes have been analyzed by

means of theoretical calculations. The obtained results show that the reaction takes place in several steps. The formation of the active species ($R_3PAuOTf$) facilitates the subsequent coordination of the alkene. Hence, once the alkene is coordinated to the gold center, the nucleophile attack can take place following an outer-sphere mechanism, with no coordination of the N -nucleophile to the metal center. Thus, this reaction goes in a different way than that proposed for the addition of methanol to propyne catalyzed by trimethylphosphane-gold(I).²⁸ In that case the O -nucleophile coordinates strongly to the metal center, whereas in this case the N -nucleophile ($CbzNH_2$) only tends to have a weak interaction with the metal. This is consistent with the experimental results, where no spectroscopically detectable interaction was found between the metal center and the substrate.¹³

The key step of the hydroamination process corresponds to the proton transfer from the NH_2 group to the unsaturated carbon atom. Theoretical calculations provided mechanistic description for this step. The calculated energy profiles indicate that direct proton transfer is characterized by a very high barrier (global barrier being 51.5 kcal/mol), which is not consistent with the mild reaction conditions. It is shown, however, that the presence

(42) That reaction consisted in the cycloisomerization of α -aminoallenes to 3-pyrrolines catalyzed by $AuCl_3$.

of OTf^- anions facilitates the heterolytic N–H bond splitting. The presence of water molecules may be also helping this process. Nevertheless, the most favorable pathway is represented by the triflate-assisted tautomerization of the “ $\text{H}_2\text{N}-\text{C}=\text{O}$ ” group followed by proton transfer from the OH group to the unsaturated carbon atom (global barrier is 26.2 kcal/mol). In principle, when there is no possibility for tautomerization, the triflate-assisted direct proton transfer also represents a considerable pathway (global barrier is 38.7 kcal/mol). Nevertheless the fact that hydroamination with simple amines, in the presence of gold complexes, is not a common process suggests that this pathway would represent an unfavorable reaction path under the generally used mild catalytic conditions.

These findings can serve as starting point and give hints for the mechanistic description of the nucleophilic additions to C–C multiple bonds, as well as to other gold(I)-catalyzed homogeneous catalytic reactions. It can be seen that the good choice of the counterion is important, since it should both form a rather weak interaction with the metal center to facilitate its substitution with the unsaturated substrate and behave as a proton shuttle facilitating the proton transfer. Moreover, it was shown by our calculations that the addition of the nucleophile is an important

factor to allow for the tautomerization by decreasing the energy difference between the tautomeric forms; the metal center is not directly involved although it facilitates the nucleophilic addition. Under investigation in our lab are other important aspects of this process, such as the origin of the regioselectivity in the hydroamination of conjugated dienes or the mechanism in the case of the addition of O-nucleophiles to alkenes.

Acknowledgment. The financial support from the Spanish MEC (Project CTQ2005-09000-CO2-01, and “Ramon y Cajal” contract to G.U.) is acknowledged. This work was also supported by the AQUACHEM Project (MCR TN-CT-2003-506864). The Catalan DURSI through Projects 2005SGR00715 and *Distinció per a la Promoció de la Recerca Universitària* to A.L. is also acknowledged.

Supporting Information Available: Cartesian coordinates and absolute energies (in gas phase and including the solvent, as well as those with the larger basis set) for the computed structures; complete ref 23. This material is available free of charge via the Internet at <http://pubs.acs.org>.

JA073578I